



An investigation of the crack propagation in tool steel X38CrMoV5 (AISI H11) in SE(T) specimens

Masood Shah, Catherine Mabru, Christine Boher, Sabine Le Roux, Farhad
Rezai-Aria

► To cite this version:

Masood Shah, Catherine Mabru, Christine Boher, Sabine Le Roux, Farhad Rezai-Aria. An investigation of the crack propagation in tool steel X38CrMoV5 (AISI H11) in SE(T) specimens. 8th International Tooling Conference (TOOL 2009), Jun 2009, Aachen, Germany. pp.1-9. hal-01691738

HAL Id: hal-01691738

<https://hal.science/hal-01691738>

Submitted on 25 Jan 2018

HAL is a multi-disciplinary open access archive for the deposit and dissemination of scientific research documents, whether they are published or not. The documents may come from teaching and research institutions in France or abroad, or from public or private research centers.




L'archive ouverte pluridisciplinaire **HAL**, est destinée au dépôt et à la diffusion de documents scientifiques de niveau recherche, publiés ou non, émanant des établissements d'enseignement et de recherche français ou étrangers, des laboratoires publics ou privés.



Open Archive TOULOUSE Archive Ouverte (OATAO)

OATAO is an open access repository that collects the work of Toulouse researchers and makes it freely available over the web where possible.

This is an author-deposited version published in : <http://oatao.univ-toulouse.fr/Eprints> ID : 2933

To cite this version : Shah, Masood and Mabru, Catherine  and Boher, Christine  and Le Roux, Sabine and Rezaï-Aria, Farhad 
An investigation of the crack propagation in tool steel X38CrMoV5 (AISI H11) in SE(T) specimens. (2009) In: TOOL 2009 - Tool steels, 2 June 2009 - 4 June 2009 (Aachen, Germany).

Any correspondence concerning this service should be sent to the repository administrator: staff-oatao@listes-diff.inp-toulouse.fr

An investigation of the crack propagation in tool steel X38CrMoV5 (AISI H11) in SE(T) specimens.

M. SHAH^a, C. MABRU^b, C. BOHER^a, S. LE ROUX^a, F. REZAÏ-ARIA^a

^a *Laboratoire Centre de Recherche, Outillages, Matériaux et Procédés (CROMeP) – Université de Toulouse, Ecole Mines Albi (EMAC).*

^b *Département Mécanique des Structures et Matériaux (DMSM), d'Institut Supérieur de l'Aéronautique et de l'Espace (ISAE)*

Keywords: Fatigue, Surface damage, Hot work tools, Crack propagation.

Abstract

A method is proposed for the evaluation of surface fatigue damage of hot forming tools that undergo severe thermo mechanical loading. Crack propagation under fatigue loading in a hot work tool steel X38CrMoV5-47HRC is investigated using specimens of 2.5*8 mm*mm section. The effect of thickness on crack propagation is investigated. The crack propagation experiments are performed at different R-values on single-edge cracked tension specimens and on specimens of different thickness. The Paris curves are established. Short crack propagation in thin specimens is also investigated. Numerical simulation and analysis of the specimens is performed by ABAQUS® Standard software. Evolution of the J integral with respect to the crack length is investigated. Crack closure along the whole crack length is observed by a microscope. Effect of slip bands on crack propagation mechanism is investigated.

1 INTRODUCTION

An approach for the study of sub-surface damage experienced in machining, tool wear, hot forming tools etc., is proposed. For example, studies on pressure die casting dies [1,2] show that the surface damage in tool steels extends from the surface down to 50-300 μm into the bulk material (this thickness will hereafter be referred to as the “surface”). It is also known that the properties of materials of low thickness may be different from those of bulk materials [3-5]. It is thus proposed to study the crack initiation and propagation behaviour of the surface separately from the bulk Figure 1. Initial results in testing procedure are presented.

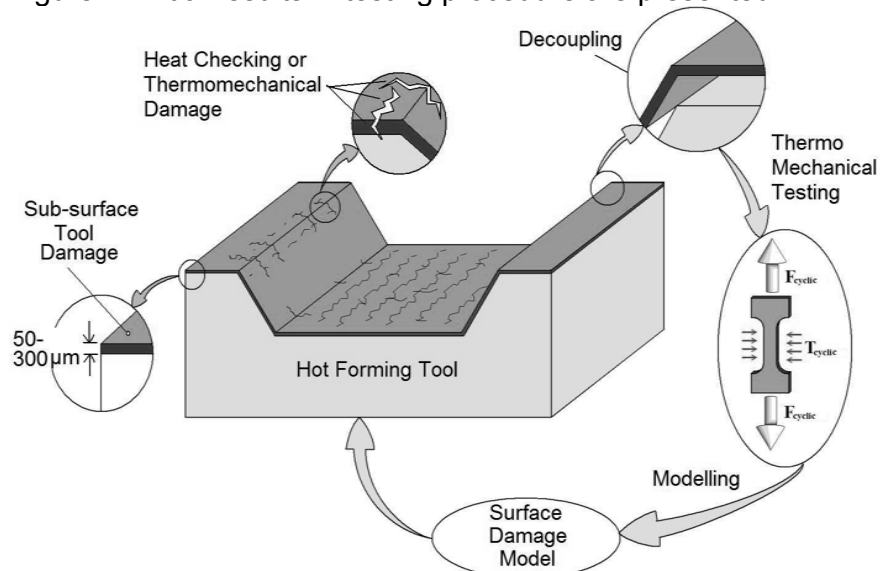


Fig. 1: General procedure for the study of surface damage in tool steels.

2 MATERIAL AND SPECIMEN PREPARATION

Material

The experiments are carried out on a hot work martensitic tool steel X38CrMoV5 (AISI H11) delivered free of charge by AUBERT & DUVAL in the form of forged bars of 60 mm square section. It is a low Si and low NMP content, 5% Chrome steel principally used in HPDC industry. The steel is quenched and double tempered to a hardness of 47 HRC and σ_y of 1000 MPa. The chemical composition by weight % is given in Table I.

Elements	C	Cr	Mn	V	Ni	Mo	Si	Fe
% Mass	0.36	5.06	0.36	0.49	0.06	1.25	0.35	bal

Table I. Chemical composition of tested steel (%weight)

Specimen Preparation and Test

All SET specimens are machined by wire cut electro erosion on an AGIECUT 100D wire cut machine Fig. 2a. The flat surfaces of the specimens are then ground parallel on an LIP 515 surface grinder. In the last stage specimens are polished on a metallographic polisher BUEHLER® PHEONIX 4000, to obtain the final thickness with a mirror finish using a 1 micrometer grit diamond paste. A grid of 0.10*0.10mm is marked on some of the specimens Fig. 2b.

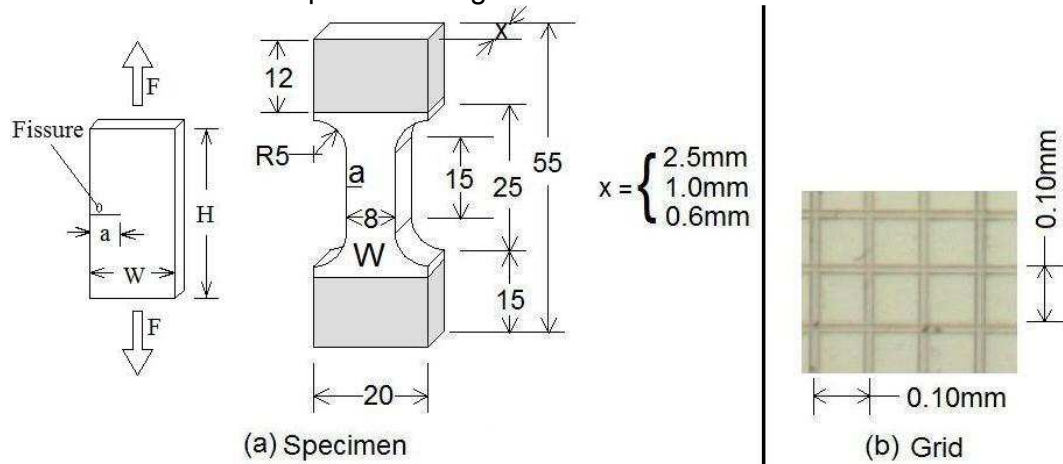


Fig 2. (a) Specimen geometry and (b) engraved grid on specimen surface.

The crack propagation experiments were carried out on a servo hydraulic universal testing machine WALTER + BAI LFV 40 at an ambient temperature of 25°C. Propagation is optically observed in situ with a QUESTAR® observation microscope (0.0012 mm resolution) without interruptions. Six different thicknesses of 2.5mm, 1.0mm, 0.6mm, 0.250mm, 0.160mm and 0.110mm were tested to evaluate the effects of thickness on the crack propagation behaviour at room temperature.

3 NUMERICAL SIMULATION

One of the main concerns in a crack propagation experiment on SET specimens is the accurate evaluation of the stress intensity factor K_I . ABAQUS® calculates the J-Integral for different values of a/W , which are used to evaluate K_I using the equation (1). An expression for correction factor $F(a/W)$ is then established by using equation (2). "E" represents the young's modulus, " σ " applied stress, "a" crack length and "W" width of specimen.

$$K_I = \sqrt{J \times E (1/\nu^2)} \quad (1)$$

$$K_I = F\left(\frac{a}{W}\right) \sigma \sqrt{\pi a} \quad (2)$$

All numerical simulation has been carried out for elastic deformation.

Verification of the K_I Calculation Procedure

The correction factor $F(a/W)$ is strongly dependent on the value of H/W . The form of the specimen being used lies between $H/W=2$ and $H/W=3$. Finite element analyses are initially carried out on standard SET specimens of $H/W=2$ Fig. 3a and $H/W=3$ Fig. 3b for range, $0.125 \leq a/W \leq 0.625$ with equal steps of 0.125. These values are then compared with those calculated by Chiodo et al. [6,7] and John et al. [8] Figure 4a.

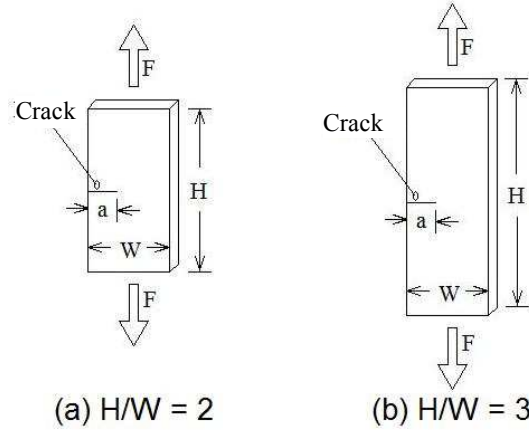


Fig. 3: Schematic of the SET standard specimens.

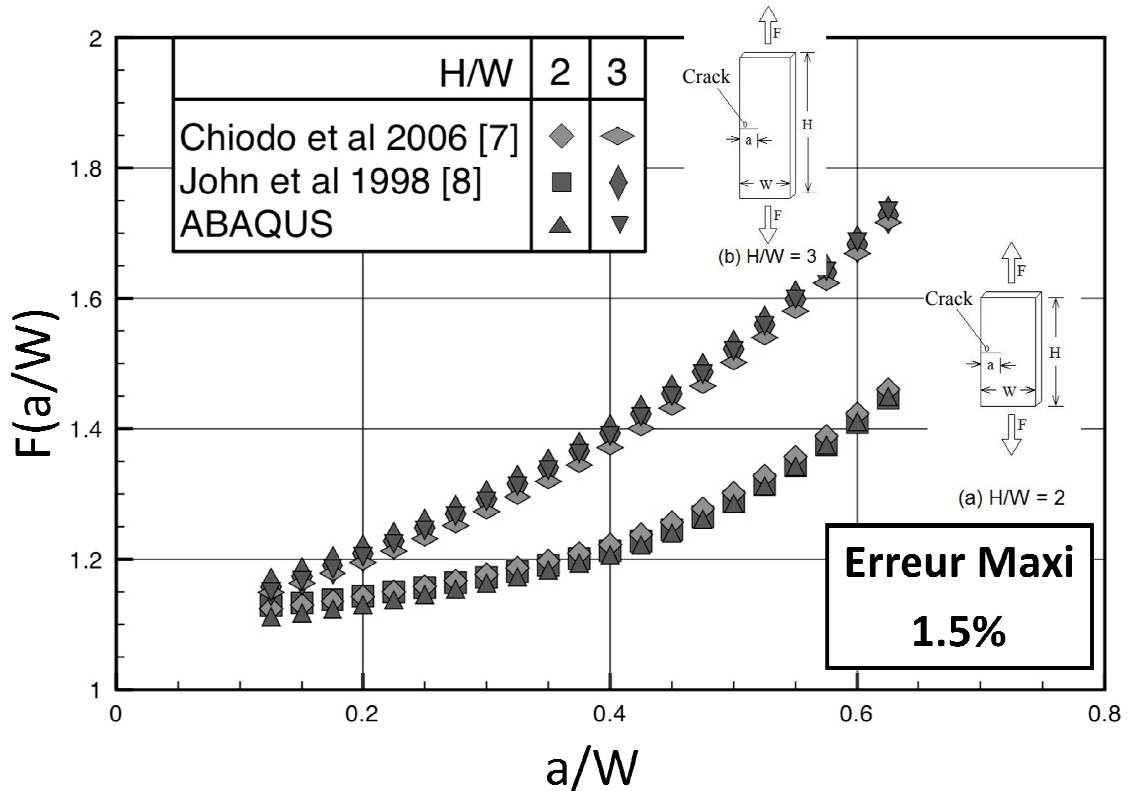


Fig. 4: Variation of correction factor $F(a/W)$ vs. a/W at two H/W ratios, comparison between ABAQUS® and [7] and [8]

The relative error is defined as: $(F_c - F_l)/F_l$, where F_c = calculated correction factor using ABAQUS® and F_l = correction factor from literature. This error in Fig. 4 does not exceed 1.5% over the whole range of crack measurement. It was therefore considered that the procedure of evaluation of K_I with ABAQUS® is relevant for the test conditions presented here.

An expression is thus obtained of $F(a/W)$ for the specimen in Fig. 2a.

$$F\left(\frac{a}{W}\right) = 1.0869 + 0.2383\left(\frac{a}{W}\right) + 1.9830\left(\frac{a}{W}\right)^2 - 2.8373\left(\frac{a}{W}\right)^3 + 2.5771\left(\frac{a}{W}\right)^4 \quad (3)$$

Equation (3) is used in conjunction with equation (2) to calculate K_I .

Calculation Procedure of K_I using ABAQUS® J-Integral

This procedure is schematically shown in Fig. 5. First, in order to define a crack, a plane partition is defined on one edge of the SET specimen, which is lengthwise centred. The edge of the plane inside the specimen defines the crack front Fig. 5-1. A region of sufficient volume is isolated around the partition. This region is fine meshed as compared to the other regions of the specimen which serves to reduce the simulation time Fig. 5-2.

Next, a cylindrical region is isolated at the crack tip Fig. 5-3. Wedge elements of type C3D15 (3D Stress wedge elements) shown in Fig. 6a are used to create the required crack tip singularity. Lastly, a larger cylinder around the crack tip is isolated and meshed using C3D20R (3D Stress, 20 node quadratic brick elements, reduced integration) elements Fig. 6b. This cylinder is used for creating the contour paths necessary to evaluate the contour integral or J values. Five contours are created around the crack front to have an effective evaluation of the plain strain K_I .

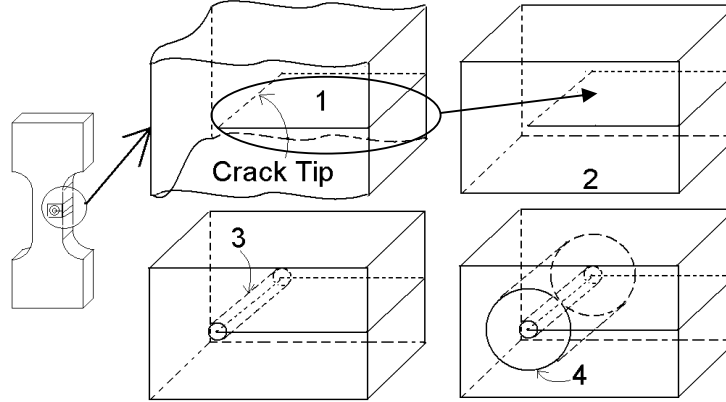


Fig. 5: Crack Modelling Procedure

Fifteen layers of elements are meshed within the thickness of the specimens. The value of J-Integral thus calculated depends on the distance of the elements from the free surfaces. An average of all values of J calculated at different depths from the free surface is taken. This average value of J is then used with equation 1 and 2 to calculate K_I and $F(a/W)$.

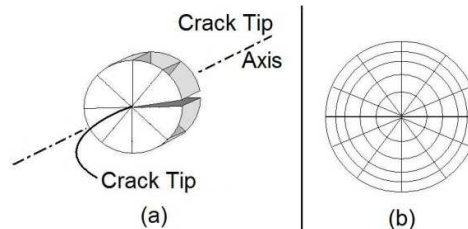


Fig. 6: (a) Wedge elements at the crack tip, (b) Contour integral meshing.

4 FATIGUE PROPAGATION AND RESULTS

The test specimens of thickness 2.5mm have been tested at two different stress ratios of $R=0.1$ and 0.7 for crack propagation, while those of thicknesses 1.0mm and 0.6mm have been tested only at $R = 0.1$. The group of thin specimens (0.250, 0.160 and 0.110mm) have been tested at different R ratios to try to establish the role of crack closure in crack propagation. Following the experiments, the Paris curves for all the specimens have been established using $\Delta a/\Delta N$ and elastic ΔK . These curves have then been compared with each other to study the effects of variability of R and of the specimen thickness. The test conditions are summarized in Table II.

Table II. Conditions for Crack Propagation Experiments

Thickness (mm)	<u>Applied stress</u> Yield stress (%)	Stress ratio $R=\sigma_{\min}/\sigma_{\max}$	Test Frequencies (Hz)
2.5	25 / 8.3	0.1	10
2.5		0.7	
1.0		0.1	
0.6	25	0.1	
0.250		0.1	
0.160		0.1	
0.110	33	0.6, 0.1	

One characteristic curve for $R=0.7$ is presented in Fig. 7. The different values of constants m and C of the Paris law [9] (equation 4) are shown on the respective graphs.

$$\frac{\Delta a}{\Delta N} = C \Delta K^m \quad (4)$$

The slope of the propagation curves tends to increase approaching threshold ΔK_I . However due to large dispersion in data the threshold values could not be clearly identified.

In the Fig. 8 a comparison is provided between $R = 0.1$ and 0.7 crack propagation rates. It is evident that the crack propagation rates tend to increase with ascending R . Also compared are the propagation curves for different thicknesses (Fig. 9) 2.5 and 0.6 mm at $R=0.1$. It can be seen that the data has a tendency to slide rightwards i.e., reduced values of crack propagation rate for the same ΔK_I . Fig. 10 provides an interesting insight into the fatigue crack propagation behaviour of thin specimens. One can see a very large increase in the threshold Stress Intensity Factor for which the crack propagation stops completely for $R = 0.1$. However this threshold seems to disappear for $R = 0.6$ even for the thinnest specimen tested at 0.110 mm thickness, and seems to approach the crack propagation curve for 2.5mm specimens.

5 FRACTOGRAPHY

Detailed post mortem fractography is carried out on the specimen crack surfaces. The specimens of 2.5mm thickness show fairly straight forward trans-granular crack propagation at first. After about 40 % advance of crack through the specimens, flat steps separated by 45° planes start to appear on the crack surfaces. These are probably related to the presence of slip bands in the deformed material beyond the crack tip. The slip bands were not visible in the 2.5mm specimens but were very clearly identified for thinner specimens (Fig. 11a) especially the 0.250mm specimen. Also the presence of the stair steps in the thinner specimens starts right from the beginning of crack propagation (Fig. 11b).

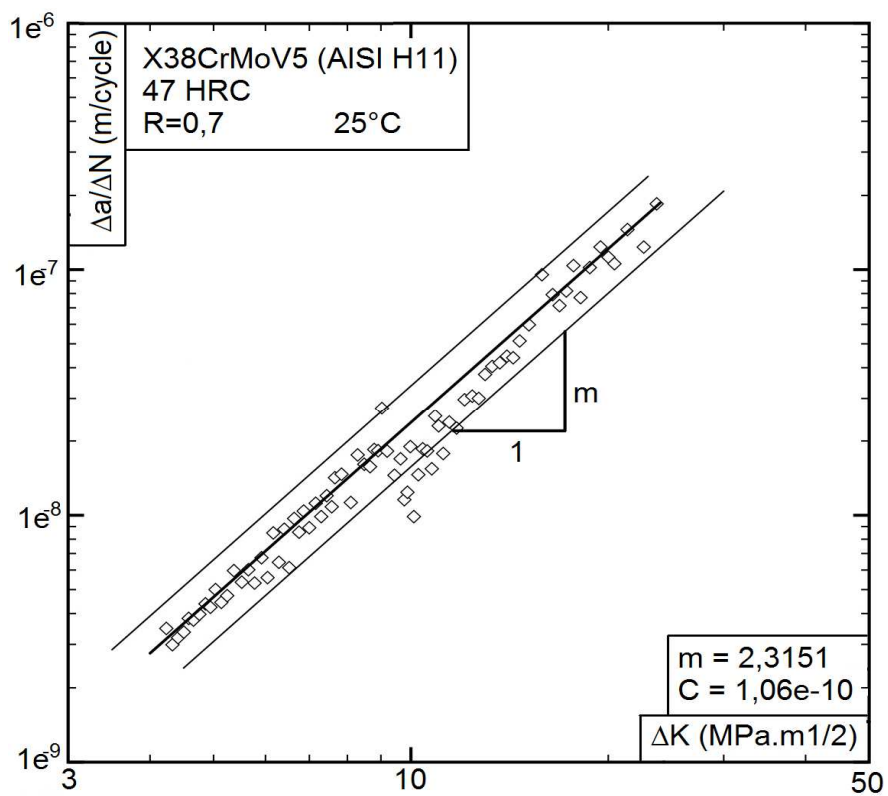


Fig. 7: Example of Paris curve for R=0.7 with thickness 2.5mm

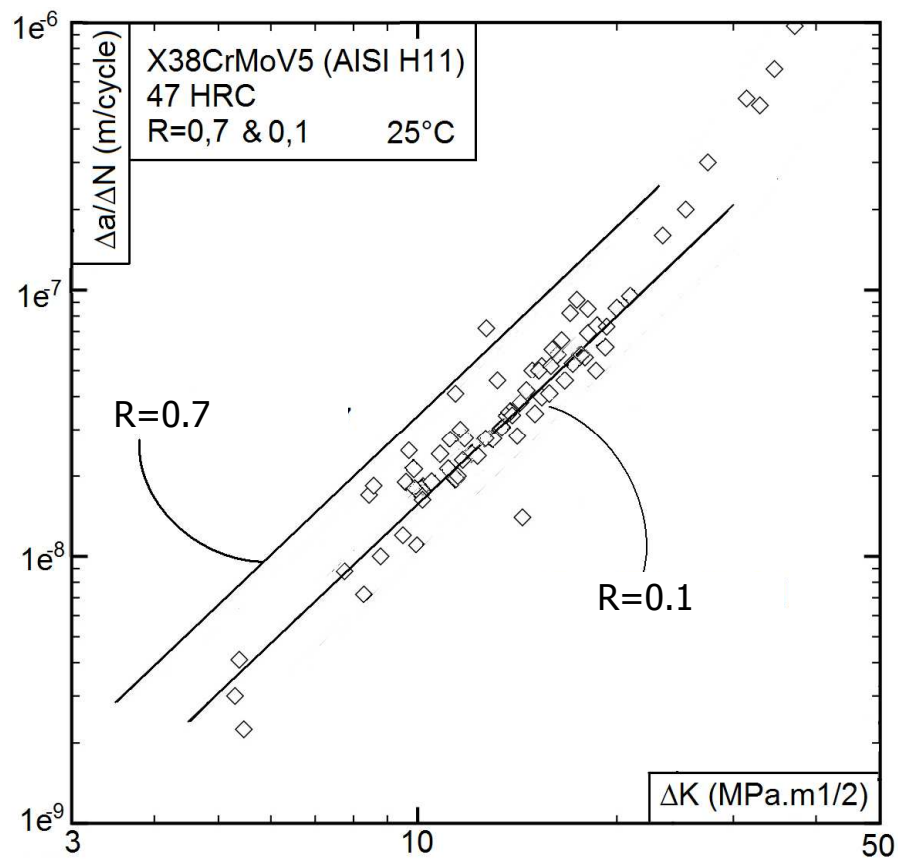


Fig. 8: Comparison of Paris curves for R=0.7 and 0.1 in 2.5mm specimen

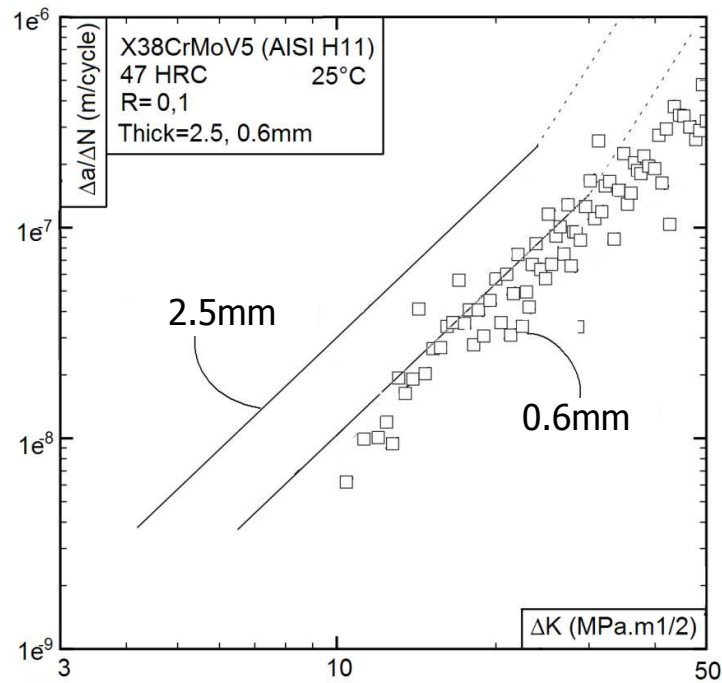


Fig. 9: Comparison of Paris curves for thickness 2.5mm and 0.6mm at R=0.1

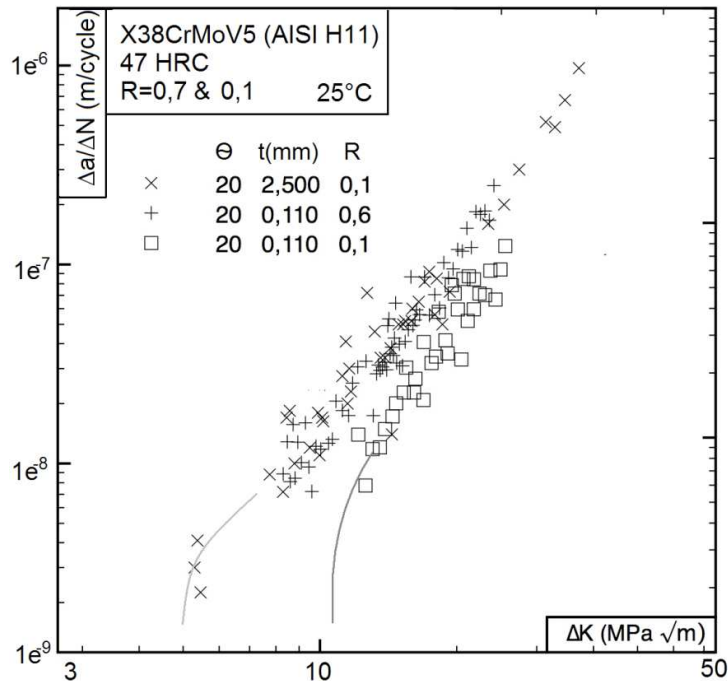


Fig. 10: Comparison of Paris curves for R=0.6 and 0.1 in 0.110mm specimen

6 DISCUSSION

For thicknesses lower than 1.0mm it seems that the testing condition approaches plane stress condition. Detailed SEM observations on thinner specimens have also revealed an important crack tip plastic zone. In the 0.250mm thickness specimen, slip bands were clearly identified on the surface, which has not previously been observed on LCF experiments on this material [10, 11] on solid cylindrical specimens. An effort was also made to measure the crack tip opening displacement and crack closure in

situ by optical measurements. At this stage no clear crack closure could be optically demonstrated.

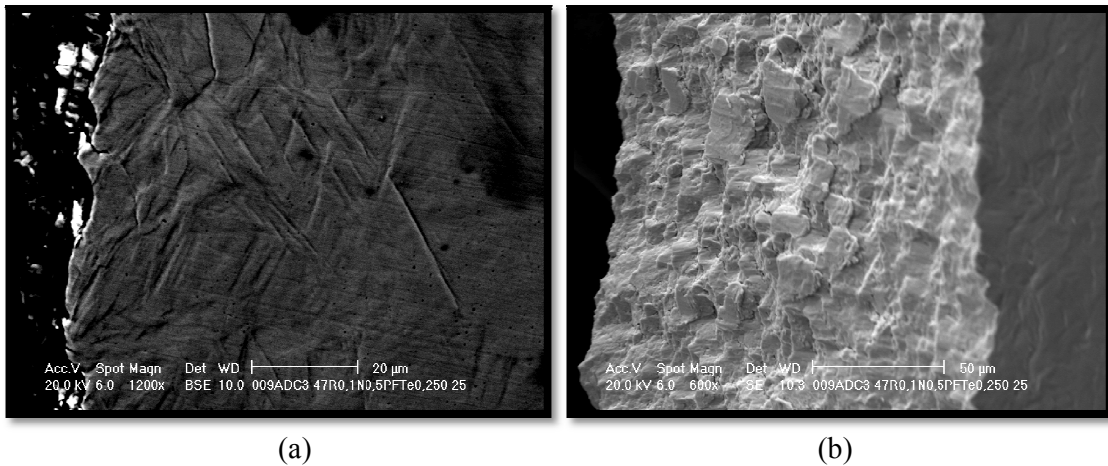


Fig. 11: SEM Micrographs of crack surfaces of 0.250mm specimen. (a) Slip bands (b) Flat steps separated by 45° planes.

The difference in the crack propagation behaviour may be explained by two reasons. First the K_{Ic} have been calculated for plane strain condition with small scale yielding. In the experiments, these conditions do not strictly prevail. In particular for specimens below 1.0mm thickness the effect of the plane stress and large plastic zone beyond the crack tip has to be considered. The second explanation could be a different crack closure mechanism due to larger plastic deformations at the crack tip of the thinner specimens compared to the 2.5mm specimen. This is fairly evident in the crack propagation curve of 0.110mm specimen (Fig. 10) the effect of crack closure can be clearly seen on the threshold value of K_{Ic} . With an increase in R from 0.1 to 0.6 the threshold value of K_{Ic} drops from around $11\text{MPa}\cdot\text{m}^{1/2}$ to $4\text{MPa}\cdot\text{m}^{1/2}$, whereas the same threshold variation for 2.5mm specimens is $5\text{MPa}\cdot\text{m}^{1/2}$ to $3\text{MPa}\cdot\text{m}^{1/2}$ for $R = 0.1$ and 0.7 respectively. The SEM micrographs of 0.250mm specimens showing presence of slip bands supports this result. More experiments will be carried out in the future to try to better understand the effect of crack closure, especially for thinner specimens.

7 CONCLUSION

Crack propagation experiments have been performed on SET specimens made of a hot work martensitic tool steel X38CrMoV5 (AISI H11). The effect of loading ratio R is studied. It is seen that the crack propagation rate increases with the increase in R . The effect of thickness on propagation rate has also been studied. A reduction in the crack propagation rates is observed with the reduction in specimen thickness. An increase in threshold K_{Ic} values is observed for $R = 0.1$ in thin specimens, however this increase seems to disappear for $R = 0.6$.

8 ACKNOWLEDGEMENTS

The authors would like to acknowledge Aubert et Duval, in particular, M. André Grellier, for providing the testing material used in this investigation free of charge.

9 REFERENCES

1. A. Persson, J. Bergström and C. Burman, 5th International Conference on Tooling, 1999, 167-177.
2. E. Ramous, A. Zambon, Proceedings of the 5th International conference on tooling, 1999, 179-184.
3. S. Hong and R. Weil, *Thin Solid Films.*, 283, 1996, 175.
4. R. Schwaiger and O. Kraft, *Scripta Materialia.*, 41(8), 1999, 823–829.
5. O. Kraft, R. Schwaiger and P. Wellner, *Mater Sci Eng.*, 2001, ,919.
6. S. Cravero and C. Ruggieri, *Engineering Fracture Mechanics.*, 74, 2007, 2735-2757.
7. M.S. Chiodo, S. Cravero, C. Ruggieri, Stress intensity factors for SE(T) specimens, Technical report, BT-PNV-68, Faculty of Engineering, University of Sao Paulo, 2006.
8. R. John and B. Rigling, *Engineering Fracture Mechanics.*, 60, 1998, 147-156.
9. P.C. Paris & F. Erdogan, *Journal of Basic Engineering.*, 85, 1963, 528-34.
10. D. Delagnes, Comportement et tenue en fatigue isotherme d'acier à outil Z 38 CDV 5 autour de la transition fatigue oligocyclique – endurance, PhD thesis, l'Ecole Nationale Supérieure des Mines de Paris., Work done at CROMeP EMAC Albi, 1998.
11. A. Oudin, Thermo-mechanical fatigue of hot work tools steels, PhD thesis, l'Ecole Nationale Supérieure des Mines de Paris., Work done at CROMeP EMAC Albi, 2001.